



ORIGINAL ARTICLE

Novel green synthesis, chemical characterization, toxicity, colorectal carcinoma, antioxidant, anti-diabetic, and anticholinergic properties of silver nanoparticles: A chemopharmacological study



Yonghong Kong^a, Bilal Ahmad Paray^{b,*}, Mohammad K. Al-Sadoon^b,
Mohammed Fahad Albeshr^b

^a Department of Pharmacy, Zhumadian Central Hospital, Zhumadian, Henan Province 463000, China

^b Department of Zoology, College of Science, King Saud University, PO Box 2455, Riyadh 11451, Saudi Arabia

Received 2 February 2021; accepted 25 April 2021

Available online 1 May 2021

KEYWORDS

Cannabis sativa L leaf;
Silver nanoparticles;
Antioxidant;
Anti-diabetic;
Anti-colorectal carcinoma

Abstract In recent research, we compared the anti-colorectal carcinoma effects of silver nanoparticles containing AgNO₃, *Cannabis sativa* L leaf aqueous extract and *C. sativa* against colorectal carcinoma in cellular models. In addition, antioxidant, anti-diabetic and anticholinergic properties of silver nanoparticles were measured. To synthesize silver nanoparticles, *C. sativa* leaf aqueous extract and AgNO₃ solutions were combined. Chemical characterization of these nanoparticles was done with TEM, FT-IR, FE-SEM, and UV-Vis. In the FT-IR assay, more antioxidant molecules with related bonds resulted in the perfect condition for the silver reduction in silver nanoparticles. The clear peak at 425 nm wavelength in UV-Vis showed the formation of silver nanoparticles. Also, in TEM and FE-SEM images, the silver nanoparticles were spherical, with an average of 11.5 nm. MTT test was used on normal (HUVEC) and colorectal carcinoma (WiDr, SW1417 [SW-1417], DLD-1, LS123, ATRFLOX [Mutatect], and Caco-2) cell lines to determine the anti-colorectal carcinoma activities of AgNO₃, *C. sativa* and silver nanoparticles. Silver nanoparticles had very low cell viability against colorectal carcinoma cell lines. The IC₅₀ of *C. sativa* and AgNPs were 603 and 379 µg/mL against the WiDr cell line, respectively; were 500 and 285 µg/mL against the SW1417 [SW-1417] cell line, respectively; were 649 and 377 µg/mL against the DLD-1 cell line, respectively; were 634 and 350 µg/mL against the LS123 cell line, respectively; were 596 and 241 µg/mL against the ATRFLOX [Mutatect] cell line, respectively; and were 539 and

* Corresponding author.

E-mail address: bparay@ksu.edu.sa (B.A. Paray).

Peer review under responsibility of King Saud University.



296 µg/mL against the Caco-2 cell line, respectively. The best result of the cytotoxicity characteristic of AgNPs against the above cell lines was seen in the case of ATRFLOX [Mutatect] cell line.

© 2021 Published by Elsevier B.V. on behalf of King Saud University. This is an open access article under the CC BY-NC-ND license (<http://creativecommons.org/licenses/by-nc-nd/4.0/>).

1. Introduction

Today, nanoparticles have become very popular due to their wide applications in biology, medicine and medicine. Structurally, their size is in the range of 100 nm (Sankar et al., 2014). There are various physical and chemical methods such as chemical reduction, photochemical reduction, ultraviolet and microwave radiation and laser for the synthesis of metallic nanoparticles. Chemical methods do not work well due to the production of toxic chemical compounds and compared to other methods, environmentally friendly bio-methods are preferred for the synthesis of metallic nanoparticles, as these methods are single-step and do not require reducing and stabilizing compounds (Baghayeri et al., 2018). Among biological methods, plants are a suitable option for the synthesis of metallic nanoparticles so that the rate of metallic ion reduction is very high. Synthesis methods by plants are low cost and high yield and lead to the production of nanoparticle crystal structures of different sizes and this depends on the nature of the plant extract, pH, temperature, and incubation time (Abdel-Fattah and Ali, 2018).

A wide range of medial supplements such as small hydrophilic and hydrophobic vaccines, drugs, and molecules of biological nanoparticles may be administered by the metallic nanoparticles (Sankar et al., 2014). They are widely used in improving the treatment and diagnosis of diseases. Nanoparticles in the form of nanofibers, carbon nanotubes, nanoliposomes, nanospheres widely have been administrated for cell scaffolding and drug carriers (Lozano, 2001; Asano, 2003; Mitrakou et al., 1998; Kimura et al., 2004). Applications of nanoparticles in drug delivery include drug carriers in disorders such as tumor, cardiovascular disease, Alzheimer's. The use of these nanocarriers is very effective for neurological diseases such as Alzheimer's because these nanoparticles can cross the blood-brain barrier due to their size that this barrier has always been a barrier to the passage of drugs to the affected area in this type of destructive brain disease (Baghayeri et al., 2018). Due to the metallic nanoparticles low size, they can also be used in brain cancers. The main aim in making metallic nanoparticles is to control the surface properties, particle size, and release of a specific and efficient drug in a specific place and time for the drug to be as effective as possible (Sankar et al., 2014; Baghayeri et al., 2018; Abdel-Fattah and Ali, 2018). Nanoparticles have many therapeutic applications and have always been used to treat various diseases. Their use in the cure of infectious, fungal, bacterial, viral, cutaneous, cardiovascular diseases has been amazing (Sankar et al., 2014). The metallic nanoparticles have unique properties to treat several cancers especially colorectal carcinoma. Metallic nanoparticles disrupt cellular communication, disrupting cellular communication networks and involved in DNA damage and in increasing the expression of the apoptotic

protein molecule and in initiating programmed cell death of apoptosis. Therefore, they lead to the proliferation of death signals, which is very important in the treatment of cancer (Sankar et al., 2014; Abdel-Fattah and Ali, 2018). In this regard, silver was previously used as a therapeutic agent. Silver nanoparticles are of great interest due to their availability, low cost, and known healing activities (Sankar et al., 2014). Among all nanoparticles, silver nanoparticles have received meticulous attention due to their wide application in chemical, optical, bioremediation, sensor, electrical, and biological field (Baghayeri et al., 2018). Silver nanoparticles synthesized by plant cells have been utilized extensively in biochemical sciences to treat more diseases. Due to the low cost and high availability of plants, the green synthesis of silver nanoparticles by medicinal plants has increased significantly. Remarkable applications of silver nanoparticles synthesized green every year are gained and this trend continues. The results of former studies have shown the important antifungal effects of silver nanoparticles synthesized by plants in the therapy of candida diseases and their antibacterial properties in the infectious treatment of *Salmonella*, *Staphylococcus*, *Streptococcus*, *Pseudomonas* and *Bacillus* (Baghayeri et al., 2018). The major therapeutic properties of silver nanoparticles are their anticancer effects. The previous study noted that silver nanoparticles had remarkable anticancer effects against various cell lines such as HCT-116 (colon cancer), HepG2 (human liver cancer), HeLa (human cervical adenocarcinoma cells), A549 (human lung carcinoma cells), SKBR3 (human breast adenocarcinoma cells), MDAMB231 (human breast adenocarcinoma), and MCF7 (human breast adenocarcinoma) (Abdel-Fattah and Ali, 2018). About the anti-acute leukemia properties of silver nanoparticles, in the previous study was revealed that polydopamine-coated silver nanoparticles had excellent anti-acute myeloid leukemia *in vitro* and *in vivo*. In the previous research, silver nanoparticles with polydopamine cap significantly abolished acute myeloid leukemia cell lines, namely Human HL-60/vcr, 32D-FLT3-ITD and Murine C1498 (Sankar et al., 2014; Abdel-Fattah and Ali, 2018). In other research, the silver nanoparticle-chitosan composite was reported to have strong anti-acute myeloid leukemia against Human HL-60/vcr, 32D-FLT3-ITD, and Murine C1498 cell lines (Baghayeri et al., 2018; Abdel-Fattah and Ali, 2018).

From ancient times and from the time when the man entered the world, he always tried to strive for a better livelihood and meet his needs. In this regard, gaining valuable experiences created only by chance has led to the use of nature around them to improve life for consecutive years (Sankar et al., 2014). The most valuable experience that is now a relic of the ancients and the wealth gained from them by modern man is the use of plants as the most natural substances around him for the treatment and even prevention of diseases, which of course is easier than cure (Baghayeri et al., 2018). The science of using medicinal plants is one of the most important

medical sciences in the world and its importance was such that some countries tried to plant and harvest some of the most important ones (Ibraheem et al., 2019). Ethnomedicinal herbs as a source of necessary chemical compositions gained much attention to treat, control, and prevent many ills and promoting body health (Rameshthangam and Chitra, 2018). Many plants are used for their antibacterial property. Due to the current progression in the herbs extraction methodology, ethnomedicinal plants are extracted in various sorts (Ibraheem et al., 2019; Rameshthangam and Chitra, 2018). One of the medicinal plant compound extraction methods used distilled water, which the produced extract is called aqueous extract (Abdel-Fattah and Ali, 2018; Ibraheem et al., 2019; Rameshthangam and Chitra, 2018). In the current years, interest in aqueous extract has been incremented for the pharmacological experiments and it appears that the aqueous extract has been useful to treat, control, and prevent animal and human bacterial infections (Sankar et al., 2014; Baghayeri et al., 2018; Abdel-Fattah and Ali, 2018; Ibraheem et al., 2019). One of the medicinal plants is *Cannabis sativa* L from the genus Rosales, family Cannabaceae and genus Cannabis. *C. sativa* in medicine, gastroprotective, hematoprotective, splenoprotective, nephroprotective, immunoprotective, hepatoprotective, antiepileptic, anti-anemic, anti-abscesses, anticancer, carminative, diuretic, cutaneous wound healing, pain relief, antipyretic, anti-parasitic, antibacterial, anti-parasitic, antifungal, antiemetic, anti-inflammatory and antioxidant effects (Lozano, 2001). The main antioxidant components of *C. sativa* are γ -tocopherol, palmitic stearic acid, oleic acid, stearidonic acid, α -linolenic acid and linoleic acid. In traditional Kurdish medicine, *C. sativa* is used to treat many cancers like breast and prostate cancers and blood diseases (Lozano, 2001).

Diabetes is a complex metabolic condition that has been partially understood until now and then provides various biochemical targets for anti-diabetic drugs. α -Glucosidase has an important place in the targets for diabetes drugs because of its integral role in the development and progression of Type 2 diabetes mellitus. Thus, α -glucosidase inhibitors are widely accepted for treating Type-2 Diabetes, effectively reducing postprandial hyperglycemia (PPGF) by delaying glucose absorption (Asano, 2003; Mitrakou et al., 1998; Kimura et al., 2004; Park et al., 2008). Accordingly, this study was conducted to evaluate the anti-colorectal carcinoma activities of silver nanoparticles conjugated with *C. sativa* aqueous extract by investigating cellular molecular approaches. On the other hand, we examined the antioxidant, antidiabetic potential of nanoparticles.

2. Experimental

2.1. Material

Phosphate buffer solution (PBS), Sabouraud Dextrose Agar, Sabouraud Dextrose Medium, Muller Hinton Agar, Mueller Hinton Medium, carbazole reagent, 4-(Dimethylamino) benzaldehyde, Dulbecco's Modified Eagle Medium (DMED), Ehrlich solution, dimethyl sulfoxide (DMSO), hydrolysate, decampmaneh fetal bovine serum, borax-sulphuric acid mixture, 2,2-diphenyl-1-picrylhydrazyl (DPPH), and antimycotic antibiotic solution all were achieved from Sigma-Aldrich company of USA.

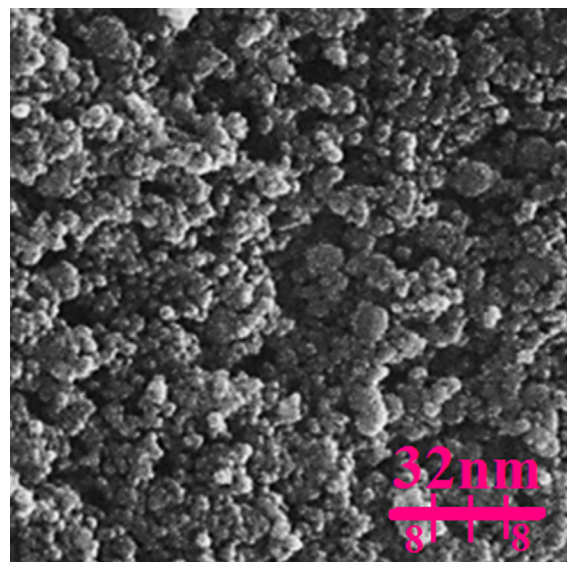


Fig. 1 FE-SEM image of AgNPs.

2.2. Synthesis of AgNPs

To obtain the aqueous extract of the plant (Fig. 1), 100 gr of the dried branches of the *C. sativa* leaves were poured in a container containing 1000 mL boiled water, and the container lid was tightly closed for 4 h. Then, the container's content was filtered, and the remaining liquid was placed on a bain-marie to evaporate. Finally, a tar-like material was obtained, which was powdered by a freeze dryer (Sankar et al., 2014).

Green synthesis of AgNPs was performed by a reaction mixture of 100 mL of AgNO₃ at a concentration of 1×10^{-3} M and a 200 mL reaction mixture of an aqueous extract solution of 1 ratio of *C. sativa* leaf (20 μ g/mL): in 10 conical flasks. The reaction mixture was kept under magnetic stirring for 12 h at room temperature. At the end of the reaction period, a black colored colloidal solution of Ag formed (Sankar et al., 2014).

Common techniques of organic chemistry, namely FT-IR and UV-Vis, to analyze AgNPs, spectroscopy, FE-SEM and TEM were used. The morphological properties of AgNPs in terms of shape and size were analyzed by FE-SEM and TEM microscopic techniques. Also, AgNPs were primarily verified using UV-Vis spectroscopy in a scanning range from 200 to 800 nm wavelength (Jasco V670 Spectrophotometer).

2.3. Assessment of cell toxicity of AgNPs

The cytotoxicity and anti-colorectal carcinoma effects of the AgNO₃, *C. sativa* and AgNPs was evaluated using MTT assay on normal (HUVEC) and colorectal carcinoma (WiDr, SW1417 [SW-1417], DLD-1, LS123, ATRFLOX [Mutatect], and Caco-2) cell lines.

At the beginning of the study, 15 mL of RPMI 1640 medium containing 10% FSC (10 mg/ml penicillin and 100 mg/ml streptomycin) in a culture flask, placed in a CO₂ incubator for 2 h to equilibrate the medium. Under safe conditions (using insulated gloves and goggles) the frozen cell vial was removed from the nitrogen storage tank. To avoid the possibility of explosion of the vial (due to the possible entry of liquid

nitrogen into the vial), loosen the lid, after disinfecting the outer surface of the vial with 70% alcohol, under the hood to remove nitrogen gas. Close the vial lid again and immediately melt it in a pan at 37 °C. The melting process should be completed in about 1 min and the cells should be avoided from overheating. The medium was added dropwise to the vial and then its contents were taken out and centrifuged with the medium in 15 cc sterile test tubes. After centrifugation, the supernatant was removed and the cells were suspended again in the medium and transferred to a pre-prepared flask containing the medium and FBS and incubated (Arulmozhi et al., 2013).

Cell line used in RPMI 1640 medium containing penicillin (100 IU/ML), streptomycin (100 IU/ML), glutamine (2 mmol) and 10% fetal bovine serum (FBS). They were incubated at 37 °C and in an atmosphere containing 0.5 CO₂. Cells began to grow in 75 cm² T-flasks in 15 mL medium with an initial number of 1–2 × 10⁶ cells. After three days and covering the flask bed with the cell, the adhesive layer to the bottom of the flask was separated enzymatically using trypsin-verseon and transferred to a sterile test tube for 10 min at 1200 rpm. The cells were then suspended in a fresh culture medium with the help of a Pasteur pipette and the suspension was poured into 100-well plate flat wells (for cell culture) using an 8-channel sampler of 100 µl. One column of wells was kept cell-free and as a plank containing only culture medium. In another column, it was considered to contain culture medium and healthy cells and in other columns, it was considered to contain culture medium and cell line cells. One of these columns, which contained culture medium and cells and did not contain AgNO₃, *C. sativa* and AgNPs, was considered as a control (Arulmozhi et al., 2013).

The plates were incubated in the incubator for 24 h to return the cells to normal from the stress of trypsinization. After this time, suitable dilutions of the prepared AgNO₃, *C. sativa* and AgNPs (0–1000 µl/ml) and 100 µl of each dilution were added columnar to the plate wells (Thus, the final concentration of the studied compound in the wells was halved. Therefore, the concentrations were prepared twice as much to reach the final concentration after being added to the well). The cells were incubated for 37 h at 37 °C and 5% CO₂ in the atmosphere. After 72 h, 20 µl of MTT solution (5 mg/ml) was added to each well. The plates were incubated for 3 to 4 h and then the residue was removed and 100 µl of DMSO was added to each well to dissolve the resulting formazan. After 10 min, using shaking the plates, the optical absorption of Formazan at 570 nm was read using a plate reader. Wells containing cells without AgNO₃, *C. sativa* and AgNPs were considered as control and the optical density of wells without cells and only culture medium were considered as blank. The percentage of cell viability was calculated using the following formula (Arulmozhi et al., 2013):

$$\text{Cell viability (\%)} = \frac{\text{Sample } A.}{\text{Control } A.} \times 100$$

The closer is the obtained value to the IC₅₀ of AgNO₃, *C. sativa* and AgNPs, the stronger is the cell viability activity of the material. The graph of the IC₅₀ of the AgNO₃, *C. sativa* and AgNPs was produced by drawing the percent inhibition curve versus the AgNO₃, *C. sativa* and AgNPs concentration.

First, three stock samples with variable concentrations (0–1000 µg/mL) of AgNO₃, *C. sativa* and AgNPs were prepared. Then, a serial dilution was prepared from each sample, and IC₅₀ of the above samples was measured separately, following which their mean was calculated (Arulmozhi et al., 2013).

2.4. Measurement of the antioxidant potential of AgNPs by DPPH

The DPPH method is a common method for assessing the antioxidant activity of plant species and metallic nanoparticles. It is based on trapping the free radicals of the material, called DPPH, using antioxidant agents that reduce the absorption rate at 517 nm wavelength. When the DPPH solution is mixed with a material that can donate hydrogen atom, radical resuscitation is formed, followed by color reduction. This reaction eliminates the purple color, whose index forms an absorption band at 517 nm (Sanchez-Moreno et al., 1998).

To determine the radical scavenging activity of the AgNO₃, *C. sativa* and AgNPs, 1 mL of 50 µM DPPH was combined with 1 mL of variable concentrations (0–1000 µg/mL) of AgNO₃, *C. sativa* and AgNPs. Then, they were transferred to the 37 °C for 1 h. The samples absorption rate was determined at 517 nm by a spectrophotometer, and the antioxidant activity was calculated by the below formula (Sanchez-Moreno et al., 1998):

$$\% \text{inhibition} = \left[\frac{(A_{\text{blank}} - A_{\text{sample}})}{A_{\text{blank}}} \right] \times 100$$

The blank sample contained 1 mL methanol and 1 mL AgNO₃, *C. sativa* and AgNPs, and a sample of 1 mL DPPH (Sanchez-Moreno et al., 1998).

Calculation of half-maximal inhibitory concentration (IC₅₀) is a suitable method for comparing the activity of pharmaceutical materials. In this method, the measurement and comparison criterion is the concentration in which 50% of the final activity of the drug occurs. In this experiment, the IC₅₀ of various repeats is estimated and compared with the IC₅₀ of BHT, which is introduced as the antioxidant activity index. The closer is the obtained value to the IC₅₀ of BHT, the stronger is the antioxidant activity of the material. The graph of the IC₅₀ of the AgNO₃, *C. sativa* and AgNPs was produced by drawing the percent inhibition curve versus the AgNO₃, *C. sativa* and AgNPs concentration. First, three stock samples with variable concentrations (0–1000 µg/mL) of AgNO₃, *C. sativa* and AgNPs were prepared. Then, a serial dilution was prepared from each sample, and IC₅₀ of the above samples was measured separately, following which their mean was calculated. BHT, with different concentrations, was considered positive control. All experiments were performed in triplicate (Sanchez-Moreno et al., 1998).

2.5. Enzymes studies

The inhibitory method of these complexes on α-glycosidase enzyme was carried out using the p-nitrophenyl-D-glycopyranoside substrate conforming to the analysis of Tao et al. (Tao et al., 2013). They were determined according to former studies (Hakamata et al., 2009; Wolffenbuttel, 1993; de Melo, 2006; Huseynova et al., 2019).

3. Results and discussion

3.1. Chemical characterization of AgNPs

Today, scanning electron microscopy is used not only in materials science, chemistry and physics, but also in many fields such as medical and biological sciences. The high resolution of SEM makes it one of the most-powerful and comprehensive tools for examining and analyzing a wide range of microstructure characteristics of samples at the nanometer to micrometer scale. Using the above technique, we can determine how the particles are placed from each other, their morphology and size (Hassan et al., 2018; Lu et al., 2021; Tian et al., 2010).

The FE-SEM image of silver nanoparticles mediated by *C. sativa* is shown in Fig. 1. AgNPs appeared as an agglomerated structure. Hydroxyl groups found in *C. sativa* may be responsible for agglomeration (Hassan et al., 2018). A similar observation, Ria et al. (2018) (Hassan et al., 2018).

One of the things that play a key role in the study of nanoparticles is determining their size. Transmission Electron Microscopy (TEM) is one of the most effective methods in determining particle size, which can provide us with useful quantitative and qualitative information (Sankar et al., 2014). The TEM test is a method that allows direct imaging of particles up to the size of an atom, and this advantage of direct imaging must be considered when working with a microscope. Appropriate qualitative analysis of nanoparticles requires optimization of different imaging methods, magnification and manual or automatic analysis methods whose purpose is to optimize the image sharpness and contrast between the sample particles and the appropriate number of particles in each image, while minimizing damage to the sample (Hassan et al., 2018; Lu et al., 2021; Tian et al., 2010). At lower image magnifications, it is possible to study the particle distribution, however, at high magnifications, a large number of particles are not observed and only information about the orientation of the plates and the structure is provided. In addition, at high magnification, high electron current causes instability and damage to the structure under study (Hassan et al., 2018; Lu et al., 2021).

In the recent study, the average size of the nanoparticles (11.5 nm) calculated through TEM images (Fig. 8). Furthermore, the histogram plot from the TEM image showed the particle size distribution of biosynthesized silver nanoparticles ranges of 8–15 nm.

In previous studies, the dimensions of silver nanoparticles formulated with an aqueous extract of medicinal plants were calculated in the spherical form in the range of 10–50 nm (Sankar et al., 2014). These reports support the results of the current study (see Fig. 2).

The method of FT-IR spectroscopy is used for detecting unknown substances, determining the quality or uniformity of the sample, determining the amount of ingredients in a mixture, identify mixtures of organic and inorganic compounds provided they are both solid or liquid, thin layer analysis, analysis of adhesives, coatings and adhesive enhancers or binders, identification of polymers and polymer mixtures, analysis of solvents, cleaners and detergents unknown, percentage of decomposition or non-polymerization of polymers and paints due to heat, UV or other factors, determination of the degree of crystallization in polymers, and analysis of resins, composite

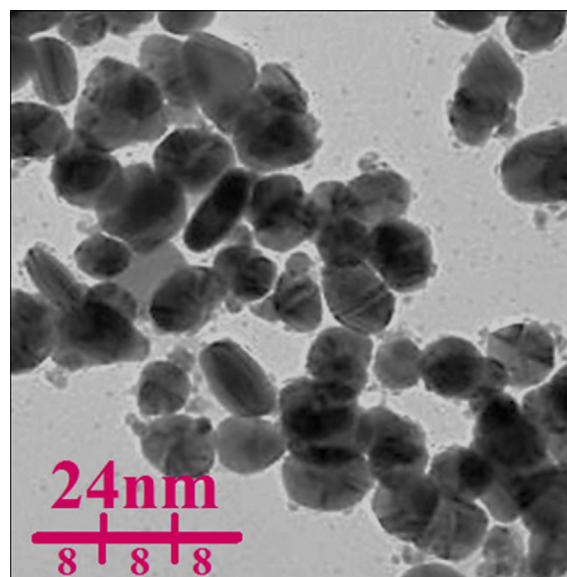


Fig. 2 TEM image of AgNPs.

materials and metal nanoparticles (Lu et al., 2021; Tian et al., 2010).

In this study, AgNPs formation confirms that Ag-O belongs to the flexural vibration with a peak at 498 cm^{-1} (Fig. 3). The IR spectroscopic method is also an adequate way to recognize bioactive ingredients in natural products. Thus, the technique is a useful method to recognize secondary metabolites of plants on AgNPs. According to the results, different IR bands related to the presence of various functional groups in *C. sativa* extract. For example, a band at 2370 cm^{-1} related to aliphatic C–H stretch; Peaks at 3436 cm^{-1} related to the O–H stretch (for alcohols, carboxylic acids and phenols); Peaks at 1018, 1100 and 1255 cm^{-1} can be attributed to the –C–O and –C–O–C stretch, and peaks at 1483, 1622 and 1697 cm^{-1} correspond to C=C and C=O phenolic and flavonoid stretching found in compounds (Lu et al., 2021; Tian et al., 2010).

UV–Visible spectroscopy is one of the techniques used in experimental sciences to obtain scientific and practical information, using the interaction of light and matter. This means that light is used in the visible and adjacent area NIRR. Absorption or reflection in the visible range directly affects the perceived rank of the chemicals involved. In this range of electromagnetic spectra are molecules under electron transfer (Hassan et al., 2018). In spectroscopy, a beam of light (beam) is shone on the material and receives information by examining the reflected or absorbed light or emission. The electromagnetic spectrum contains a range of wavelengths. Each region of this spectrum has a special name, such as infrared, far-infrared, near-infrared, and X-rays. The range of 400–800 nm is called the visible range and 200–400 nm is called the ultraviolet range. UV–Visible spectroscopy studies this area (Lu et al., 2021; Tian et al., 2010).

Fig. 4 shows an absorption band at 425 nm for the surface plasmon resonance of AgNPs. We can also find that by increasing the amount of *C. sativa* extract solution, the density of the SPR band increases. Using a higher concentration of *C. sativa* extract indicates that the average AgNP size decreased and the AgNP concentration increased.

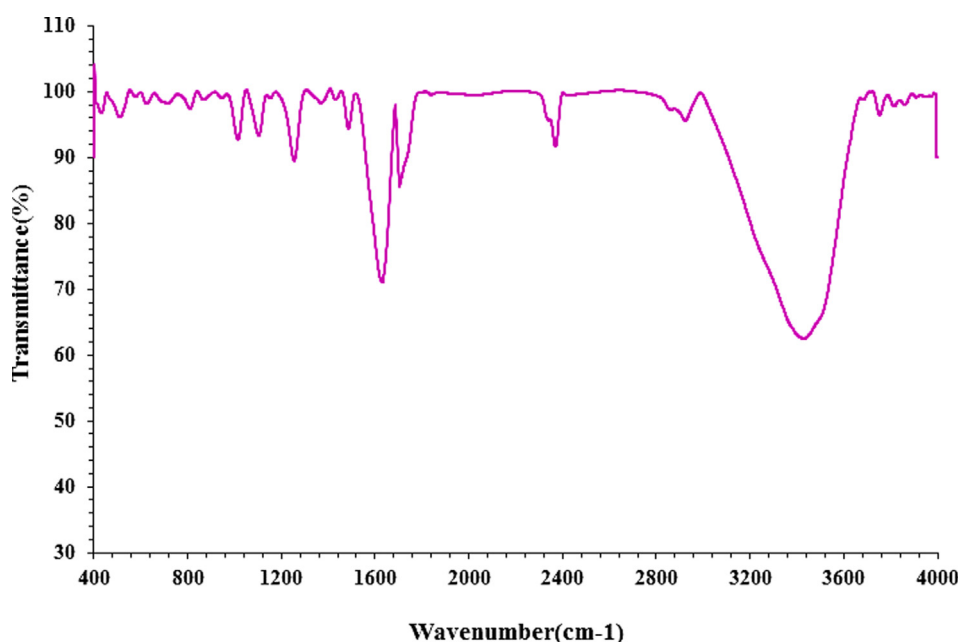


Fig. 3 FT-IR spectra of biosynthesized AgNPs.

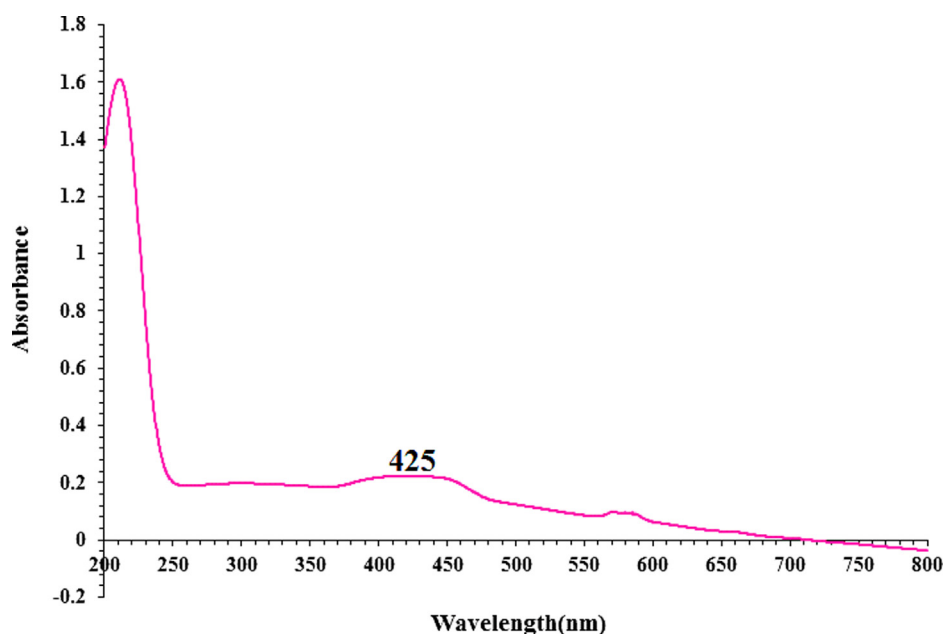


Fig. 4 UV-Vis spectra of biosynthesized AgNPs.

3.2. Cytotoxicity and anticancer potentials of AgNPs

The MTT assay is a procedure of colorimetric based on reducing and breaking of yellow tetrazolium crystals by the enzyme succinate dehydrogenase to form insoluble purple crystals. In this method, unlike other methods, the steps of washing and collecting cells, which often cause the loss of a number of cells and increase the work error, have been eliminated and all test steps from the beginning of cell culture to reading the results with a photometer are performed on a microplate, so the repeatability, accuracy and sensitivity of the test are high

(Sankar et al., 2014; Baghayeri et al., 2018). If the test is performed on cells attached to the plate, an appropriate number of cells (about 2000 cells) must first be cultured in each of the wells. Then we select the control and test wells and add the appropriate amount of mitogen or drug to the test wells and place the plate in the incubator for the required time so that the desired substance affects the cells (Abdel-Fattah and Ali, 2018). At the end of the incubation time, discard the supernatant and add 200 μ l of culture medium containing half an mg/ml of MTT solution to each well and put it again in a carbon dioxide incubator for 2 to 4 h at 37 $^{\circ}$ C. During incuba-

tion, MTT is regenerated by one of the enzymes of the mitochondrial respiratory cycle i.e., succinate dehydrogenase. The regeneration and breakage of this ring produce purple-blue crystals of formazan that are easily detectable under a microscope (Baghayeri et al., 2018; Abdel-Fattah and Ali, 2018; Ibraheem et al., 2019). At the end, the optical absorption of the resulting solution can be read at 570 nm and the cells number can be calculated using a standard curve. For each cell line, there is a linear relationship between the number of cells and the light absorption of the final solution. Therefore, to examine each cell type, a standard curve related to the same cell line must be drawn and used (Arulmozhi et al., 2013).

In the recent study, treated cells with various concentrations of AgNO₃, *C. sativa* and AgNPs were examined for cytotoxicity on normal (HUVEC) and colorectal carcinoma (WiDr, SW1417 [SW-1417], DLD-1, LS123, ATRFLOX [Mutatect], and Caco-2) cell lines by 48 h MTT assay (Figs. 5–8). The absorbance rate was determined at 570 nm, which showed exceptional viability for AgNO₃, *C. sativa* and AgNPs even up to 1000 µg/mL in the normal cell line (HUVEC).

In the case of colorectal carcinoma cell lines their viability decreased in a dose-dependent manner in the presence of AgNO₃, *C. sativa* and AgNPs. The IC₅₀ of *C. sativa* and AgNPs were 603 and 379 µg/mL against the WiDr cell line, respectively; were 500 and 285 µg/mL against the SW1417 [SW-1417] cell line, respectively; were 649 and 377 µg/mL against the DLD-1 cell line, respectively; were 634 and 350 µg/mL against the LS123 cell line, respectively; were 596 and 241 µg/mL against the ATRFLOX [Mutatect] cell line, respectively; and were 539 and 296 µg/mL against the Caco-2 cell line, respectively. The best result of the cytotoxicity characteristic of AgNPs against the above cell lines was seen in the case of ATRFLOX [Mutatect] cell line.

In several studies, agreement with our experiment has shown the excellent anticancer potential of biosynthesized AgNPs using *Piper longum* leaf extracts against cervical cell lines (HeLa) (Suman et al., 2013) and *Morinda citrifolia* against liver cancer cell line (Hep-2) (Vivek et al., 2012; You et al., 2012).

It was found that the anticancer of silver nanoparticles is highly dependent on a number of factors related to their physical properties such as surface coating, shape and size.

It has been reported that small sized silver nanoparticles can transfer and remove the cell membrane of tumor cells.

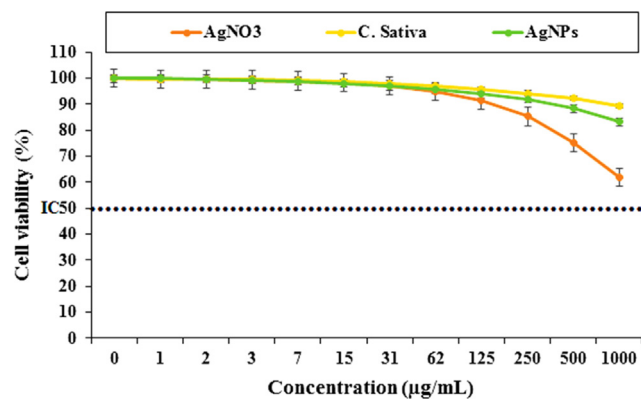


Fig. 5 Percent viability measured on HUVEC after treatment with present AgNO₃, *C. sativa*, and AgNPs.

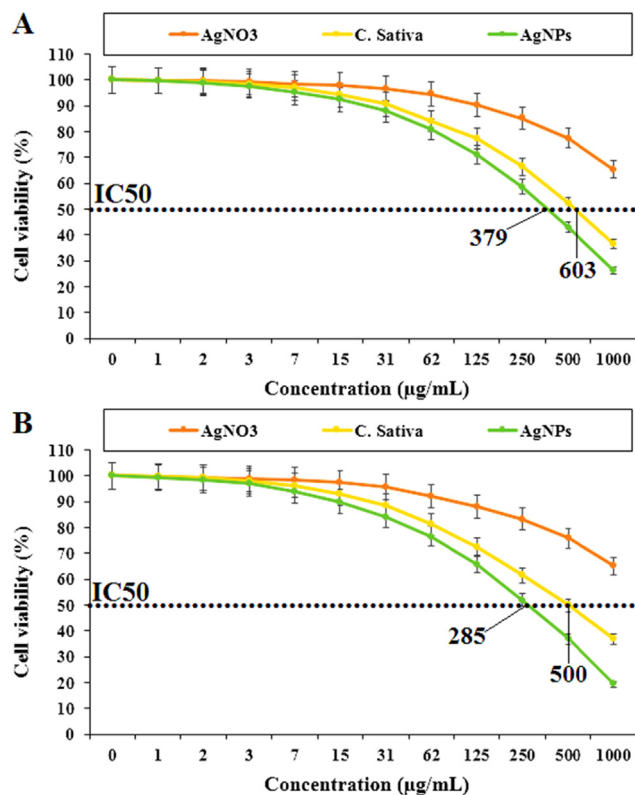


Fig. 6 Percent viability measured on colorectal carcinoma cell lines including WiDr (A) and SW1417 [SW-1417] (B) after treatment with present AgNO₃, *C. sativa*, and AgNPs.

At a larger size, the above capability is significantly limited (Namvar et al., 2014). As shown in Figs. 7 and 8 of our study, silver nanoparticles had a uniform spherical morphology in the 8–15 nm range. The size of silver nanoparticles below 50 nm is well suited for killing tumor cell lines (Namvar et al., 2014).

3.3. Antioxidant potential of AgNPs

Free radicals are molecules that do not have a complete electron shell, which increases the chemical reaction relative to others. Free radicals are formed if you are exposed to tobacco smoke and radiation. In humans, the most important free radical is oxygen. When an oxygen molecule (O₂) is exposed to radiation, it removes an electron from the other molecules, destroying DNA and other molecules (Abdel-Fattah and Ali, 2018; Ibraheem et al., 2019; Rameshthangam and Chitra, 2018). Some of these changes cause disease. Problems such as heart problems, muscle failure, diabetes and cancer are all caused by these free radicals. Antioxidants act like a broom against free radicals, destroying free radicals and regenerating damaged cells. Laboratory evidence has shown that antioxidants can prevent cancer (Sankar et al., 2014; Baghayeri et al., 2018).

Plants have excellent antioxidant capacity. One way to increase the antioxidant capacity of plants is to combine them with metallic salts. In previous studies, it was revealed that their antioxidant activities were significantly increased when plants were combined with zinc, copper, silver, titanium, iron, and gold (Matthaus, 2002).

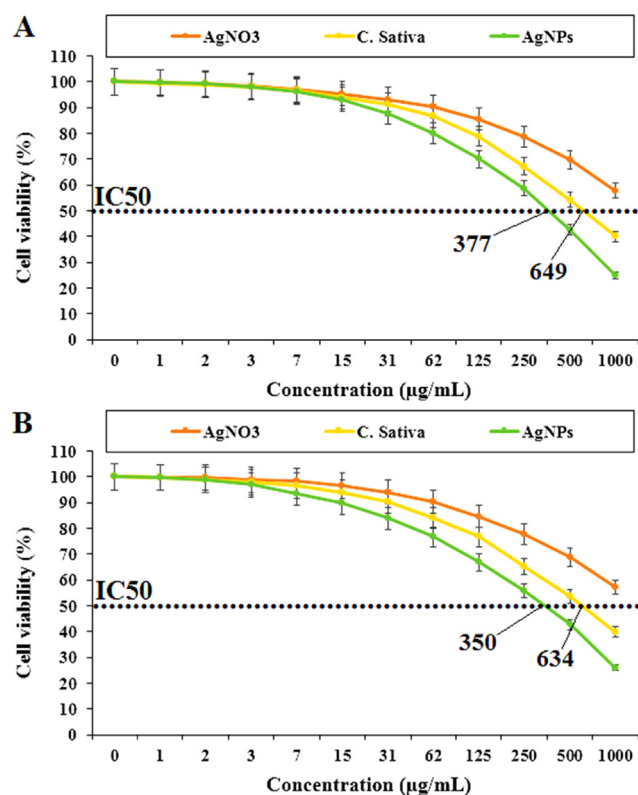


Fig. 7 Percent viability measured on colorectal carcinoma cell lines including DLD-1 (A) and LS123 (B) after treatment with present AgNO₃, *C. sativa*, and AgNPs.

In our study, *C. sativa* extract and AgNPs similar to BHT showed a remarkable concentration-dependent DPPH radical scavenging effect (Ibraheem et al., 2019). IC₅₀ values of *C. sativa*, BHT and AgNPs were 339, 301, and 218 µg/mL, respectively (Fig. 9).

Previous work determined that *C. sativa* is rich in antioxidant compounds such as oleic acid, stearidonic acid, α -linolenic acid, tocopherol, palmiticstearic acid, and linoleic acid (Matthaus, 2002; Ishino and Wakita, 2010; Lozano, 2001).

Oxidation from reactive oxygen species can cause cell membrane disintegration, damage to membrane proteins, and DNA mutation that the result is the onset or exacerbation of many diseases such as cancer, liver damage, and cardiovascular disease. Although the body has a defense system, constant exposure to chemicals and contaminants can lead to an increase in the number of free radicals outside the body's defense capacity and irreversible oxidative damage (Katata-Seru et al., 2018; Sangami and Manu, 2017; Beheshtkhoo et al., 2018). Therefore, antioxidants with the property of removing free radicals play an important role in the prevention or treatment of oxidation-related diseases or free radicals. Extensive molecular cell research on cancer cells has developed a targeted approach to the biochemical prevention of cancers that the goal is to stop or return cells to their pre-cancerous state without any toxic doses through nutrients and drugs (Katata-Seru et al., 2018; Radini et al., 2018). Numerous studies have been performed on using natural compounds as anti-cancer agents in relation to appropriate antioxidant activity (Radini et al., 2018; Oganessian et al., 1991; Ramyadevi

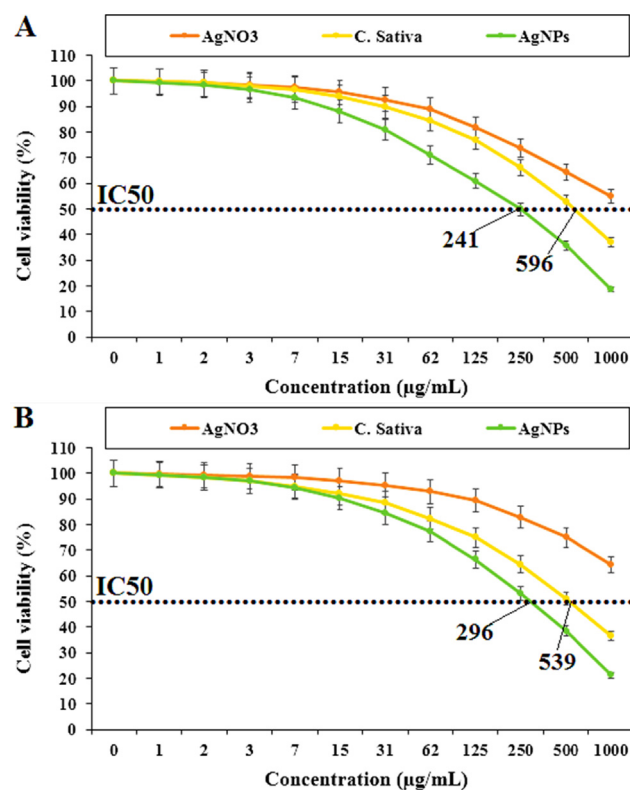


Fig. 8 Percent viability measured on colorectal carcinoma cell lines including ATRFLOX [Mutatec] (A) and Caco-2 (B) after treatment with present AgNO₃, *C. sativa*, and AgNPs.

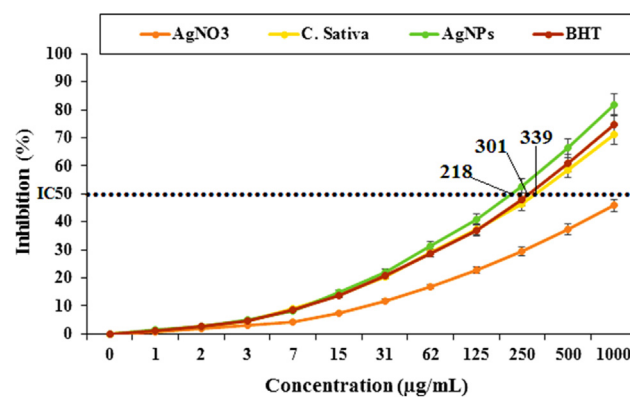


Fig. 9 Antioxidant potential of AgNO₃, *C. sativa*, AgNPs, and BHT.

et al., 2012). It seems the high anti-lung adenocarcinoma properties of *C. sativa* and silver nanoparticles are related to its antioxidant activities.

3.4. Enzymes results

3.4.1. α -Glycosidase inhibition results

For the enzyme glycosidase, the IC₅₀ values of the new silver nanoparticles are 32.31 and 85.35 micromolar and Ki values 39.43 ± 7.31 and 125.30 ± 12.64 micromolar (Table 1). The results documented that all these new compounds demonstrate the inhibitory effects of α -glycosidase acarbose (IC₅₀:

Table 1 Inhibition results of important enzyme (IC₅₀ ve Ki values).

AgNO ₃	Enzyme	α -Gly (μ M)
	IC ₅₀	85.35
	Ki + std	125.30 + 12.64
AgNPs	IC ₅₀	32.31
	Ki + std	39.43 \pm 7.31
Standard (Acarbose)	IC ₅₀	133.34
	Ki + std	153.23 \pm 13.08

133.34 micromolar) as a standard glycosidase inhibitor. In fact, the most effective Ki of AgNPs was 39.43 micromolar, respectively. For α -glycosidase, IC₅₀ values of ACR as positive control and the following order for some novel compounds: AgNPs (32.31 micromolar) < AgNO₃ (85.35 micromolar) < ACR (133.34 micromolar). α -Glycosidase inhibitors can delay carbohydrate digestion and extend overall carbohydrate digestion time, thus helping to lower post-meal blood sugar levels. These inhibitors such as acarbose, vogomibose, and miglitol have been used in the clinical setting as first-line treatments for type 2 diabetes. Unfortunately, these treatments can cause side effects such as diarrhea, bloating, and abdominal pain. Therefore, the discovery of safe and effective enzyme inhibitors is required for effective control of diabetic disorders. (Saludes et al., 2007; Seo et al., 2005).

4. Conclusion

In the last research, the collected Cannabis sativa L leaf was applied for the biosynthesis of silver nanoparticles. After the silver nanoparticles are synthesized, FE-SEM, TEM, UV vis. And it was characterized by FT-IR. In cellular models of this experiment, silver nanoparticles revealed significant anti-colorectal carcinoma activities against colorectal carcinoma cell lines. In vivo and clinical trials are recommended to confirm the above effects in humans. We also investigated the inhibitory activity of silver nanoparticles against α -glucosidase. As a result of this work, the new silver nanoparticles showed micromolar levels of inhibition against these enzymes. The newly synthesized nanoparticles were good inhibitors for the α -glucosidase enzyme.

Declaration of Competing Interest

The authors declare that they have no known competing financial interests or personal relationships that could have appeared to influence the work reported in this paper.

Acknowledgement

The authors would like to extend their sincere appreciation to the Deanship of Scientific Research at the King Saud University, Riyadh, Saudi Arabia for funding this Research Group Project No. RG-1437-005.

References

Abdel-Fattah, W.I., Ali, G.W., 2018. Anti-Cancer Activities of Silver Nanoparticles. *J Appl Biotechnol Bioeng.* 5, 00116.

- Arulmozhi, V., Pandian, K., Mirunalini, S., 2013. Ellagic acid encapsulated chitosan nanoparticles for drug delivery system in human oral cancer cell line (KB). *Colloids. Surf. B: Biointerfaces.* 110, 313–320.
- Asano, N., 2003. Glycosidase Inhibitors: update and Perspectives on Practical Use. *Glycobiology* 13 (10), 93R–104R.
- Baghayeri, M., Mahdavi, B., Hosseinpour-Mohsen Abadi, Z., Farhadi, S., 2018. Green synthesis of silver nanoparticles using water extract of *Salvia leriifolia*: Antibacterial studies and applications as catalysts in the electrochemical detection of nitrite. *Applied Organometallic Chemistry* 32, e4057.
- Beheshtkhoo, N., Kouhbanani, M.A.J., Savardashtaki, A., Amani, A. M., Taghizadeh, S., 2018. Green synthesis of iron oxide nanoparticles by aqueous leaf extract of *Daphne mezereum* as a novel dye removing material. *Appl Phys A.* 124, 363–369.
- de Melo, E.B., da Silveira Gomes, A., Carvalho, I., 2006. α - and β -Glycosidase Inhibitors: chemical Structure and Biological Activity. *Tetrahedron* 62 (44), 10277–10302.
- Hakamata, W., Kurihara, M., Okuda, H., Nishio, T., Oku, T., 2009. Design and Screening Strategies for Alpha-Glucosidase Inhibitors Based on Enzymological Information. *Current Topics in Medicinal Chemistry* 9 (1), 3–12.
- Hassan, S.E., Salem, S.S., Fouda, A., Awad, M.A., El-Gamal, M.S., Abdo, A.M., 2018. Endophytic actinomycetes *Streptomyces* spp mediated biosynthesis of copper oxide nanoparticles as a promising tool for biotechnological applications. *J Radiat Res Diat Res Appl Sci.* 3, 262–270.
- Huseynova, M., Medjidov, A., Taslimi, P., Aliyeva, M., 2019. Synthesis, Characterization, Crystal Structure of the Coordination Polymer Zn(II) with Thiosemicarbazone of Glyoxalic Acid and Their Inhibitory Properties Against Some Metabolic Enzymes. *Bioorg Chem.* 83, 55–62.
- Ibraheem, F., Aziz, M.H., Fatima, M., Shaheen, F., Ali, S.M., Huang, Q., 2019. In vitro Cytotoxicity, MMP and ROS activity of green synthesized nickel oxide nanoparticles using extract of *Terminalia chebula* against MCF-7 cells. *Materials Letters* 234, 129–133.
- Ishino, K.C., Wakita, T., 2010. Shibata, Lipid Peroxidation Generates Body Odor Component trans-2-Nonenal Covalently Bound to Protein in Vivo. *J Biol Chem.* 285, 15302–15313.
- Katata-Seru, L., Moremedi, T., Aremu, O.S., Bahadur, I., 2018. Green synthesis of iron nanoparticles using *Moringa oleifera* extracts and their applications: Removal of nitrate from water and antibacterial activity against *Escherichia coli*. *J Mol Liq.* 256, 296–304.
- Kimura, A., Lee, J.-H., Lee, I.-S., Lee, H.-S., Park, K.-H., Chiba, S., Kim, D., 2004. Two Potent Competitive Inhibitors Discriminating Alpha-Glucosidase Family I from Family II. *Carbohydrate Research* 339 (6), 1035–1040.
- Lozano, I., 2001. The Therapeutic Use of Cannabis sativa (L.) in Arabic Medicine. *J Cannabis Therap.* 1, 63–70.
- Lu, Y., Wan, X., Li, L., Sun, P., Liu, G., 2021. Synthesis of a reusable composite of graphene and silver nanoparticles for catalytic reduction of 4-nitrophenol and performance as anti-colorectal carcinoma. *Journal of Materials Research and Technology.* 12, 1832–1843.
- Matthaus, B., 2002. Antioxidant activity of extracts obtained from residues of different oilseeds. *J Agric Food Chem* 50, 3444–3452.
- Mitrakou, A., Tountas, N., Raptis, A., Bauer, R., Schulz, H., Raptis, S., 1998. Long-Term Effectiveness of a New α -Glucosidase Inhibitor (Bay m1099-Miglitol) in Insulin-Treated Type 2 Diabetes Mellitus. *Diabetic Medicine* 15 (8), 657–660.
- Namvar, F., Rahman, H.S., Mohamad, R., Baharara, J., Mahdavi, M., Amini, E., Chartrand, M.S., Yeap, S.K., 2014. Cytotoxic effect of magnetic iron oxide nanoparticles synthesized via seaweed aqueous extract. *Int J Nanomedicine.* 19, 2479–2488.

- Oganesvan, G., Galstyan, A., Mnatsakanyan, V., Paronikyan, R., Ter-Zakharyan, Y.Z., 1991. Phenolic and flavonoid compounds of *Ziziphora clinopodioides*. *Chem Nat.* 27, 247-247.
- Park, H., Hwang, K.Y., Oh, K.H., Kim, Y.H., Lee, J.Y., Kim, K., 2008. Discovery of Novel Alpha-Glucosidase Inhibitors Based on the Virtual Screening with the Homology-Modeled Protein Structure. *Bioorganic & Medicinal Chemistry* 16 (1), 284-292.
- Radini, I.A., Hasan, N., Malik, M.A., Khan, Z., 2018. Biosynthesis of iron nanoparticles using *Trigonella foenum-graecum* seed extract for photocatalytic methyl orange dye degradation and antibacterial applications. *J Photochem Photobiol B.* 183, 154-163.
- Rameshthangam, P., Chitra, J.P., 2018. Synergistic anticancer effect of green synthesized nickel nanoparticles and quercetin extracted from *Ocimum sanctum* leaf extract. *Journal of materials science & technology* 34, 508-522.
- Ramyadevi, J., Jeyasubramanian, K., Marikani, A., Rajakumar, G., Rahuman, A.A., 2012. Synthesis and Antimicrobial Activity of Copper Nanoparticles. *Mater lett.* 71, 114-116.
- Saludes, J.P., Lievens, S.C., Molinski, T.F., 2007. Occurrence of the Alpha-Glucosidase Inhibitor 1,4-Dideoxy-1,4-imino-D-arabinitol and Related Iminopentitols in Marine Sponges. *Journal of Natural Products* 70 (3), 436-438.
- Sanchez-Moreno, C., Larrauri, J.A., Saura-Calixto, F., 1998. A procedure to measure the antiradical efficiency of polyphenols. *J Sci Food Agric.* 76, 270-276.
- Sangami, S., Manu, B., 2017. Synthesis of Green Iron Nanoparticles using Laterite and their application as a Fenton-like catalyst for the degradation of herbicide Ametryn in water. *Environ Technol Innov.* 8, 150-163.
- Sankar, R., Maheswari, R., Karthik, S., et al, 2014. Anticancer activity of *Ficus religiosa* engineered copper oxide nanoparticles. *Mat Sci Eng C* 44, 234-239.
- Seo, W.D., Kim, J.H., Kang, J.E., Ryu, H.W., Curtis-Long, M.J., Lee, H.S., Yang, M.S., Park, K.H., 2005. Sulfonamide Chalcone as a new class of alpha-glucosidase inhibitors. *Bioorg. Med. Chem. Lett.* 15 (24), 5514-5516.
- Suman, T.Y., Rajasree, S.R., Kanchana, A., Elizabeth, S.B., 2013. Biosynthesis, characterization and cytotoxic effect of plant mediated silver nanoparticles using *Morinda citrifolia* root extract. *Colloids. Surf. B. Biointerfaces* 106, 74-78.
- Tao, Y., Zhang, Y., Cheng, Y., 2013. Rapid screening and identification of α -glucosidase inhibitors from mulberry leaves using enzyme-immobilized magnetic beads coupled with HPLC/MS and NMR. *Biomed. Chrom.* 27, 148-155.
- Tian, S., Shi, Y., Yu, Q., Upur, H., 2010. Determination of oleanolic acid and ursolic acid contents in *Ziziphora clinopodioides* Lam. by HPLC method. *Pharmacog Mag.* 6, 116-119.
- Vivek, R., Thangam, R., Muthuchelian, K., Gunasekaran, P., Kaveri, K., Kannan, S., 2012. Green biosynthesis of silver nanoparticles from *Annona squamosa* leaf extract and its in vitro cytotoxic effect on MCF-7 cells. *Process. Biochem.* 47, 2405-2410.
- Wolffenbuttel, B., 1993. Type 2 Diabetes Mellitus. *The Netherlands Journal of Medicine* 43 (3-4), 187-199.
- You, C., Han, C., Wang, X., Zheng, Y., Li, Q., Hu, X., Sun, H., 2012. The progress of silver nanoparticles in the antibacterial mechanism, clinical application and cytotoxicity. *Mol. Biol. Rep.* 39, 9193-9201.